

RESEARCH ARTICLE

Environmental entrainment demonstrates natural circadian rhythmicity in the cnidarian *Nematostella vectensis*

Ann M. Tarrant^{1,*}, Rebecca R. Helm^{1,2}, Oren Levy³ and Hanny E. Rivera^{1,4}

ABSTRACT

Considerable advances in chronobiology have been made through controlled laboratory studies, but distinct temporal rhythms can emerge under natural environmental conditions. Lab-reared *Nematostella vectensis* sea anemones exhibit circadian behavioral and physiological rhythms. Given that these anemones inhabit shallow estuarine environments subject to tidal inputs, it was unclear whether circadian rhythmicity would persist following entrainment in natural conditions, or whether circatidal periodicity would predominate. *Nematostella* were conditioned within a marsh environment, where they experienced strong daily temperature cycles as well as brief tidal flooding around the full and new moons. Upon retrieval, anemones exhibited strong circadian (~24 h) activity rhythms under a light–dark cycle or continuous darkness, but reduced circadian rhythmicity under continuous light. However, some individuals in each light condition showed circadian rhythmicity, and a few individuals showed circatidal rhythmicity. Consistent with the behavioral studies, a large number of transcripts (1640) exhibited diurnal rhythmicity compared with very few (64) with semidiurnal rhythmicity. Diurnal transcripts included core circadian regulators, and 101 of 434 (23%) genes that were previously found to be upregulated by exposure to ultraviolet radiation. Together, these behavioral and transcriptional studies show that circadian rhythmicity predominates and suggest that solar radiation drives physiological cycles in this sediment-dwelling subtidal animal.

KEY WORDS: Chronobiology, Circadian, Cnidarian, Entrainment, Subtidal, UV radiation

INTRODUCTION

Endogenous timing mechanisms enable organisms to anticipate and prepare for predictable environmental changes. Among these, photoperiodic entrainment of the daily or circadian clock has been intensely studied, the underlying molecular machinery has been elucidated in a few model species, and core aspects have been shown to be conserved across diverse animal lineages. Throughout the manuscript ‘circadian’ and ‘circatidal’ are used to describe ~24 h and ~12.4 h rhythms demonstrated to persist under constant light and temperature conditions; ‘diurnal’ or ‘semidiurnal’ are used more generally to describe rhythms with corresponding periodicity


that may or may not be endogenously regulated. While controlled laboratory conditions provide a necessary foundation for mechanistic studies, the ecologically relevant temporal cycles for an organism are influenced by interactions between distinct abiotic cycles (e.g. photoperiod, tidal fluctuations), as well as biotic cycles (e.g. food availability, predation pressure; reviewed by Helm et al., 2017). Accordingly, studies in diverse species of wild animals or animals reared under more realistic conditions have indeed revealed new aspects of temporal regulation. For example, under natural light and temperature conditions, *Drosophila melanogaster* exhibits a pronounced afternoon activity peak rather than the low-activity ‘siesta’ period that is observed in typical laboratory conditions (constant temperature and a binary on/off light cycle; Vanin et al., 2012). A study of subterranean rodents in semi-natural enclosures revealed substantial aboveground burrowing activity during daytime hours, whereas lab-reared animals were strictly nocturnal (Tomotani et al., 2012). Circadian cycles of honeybees are strongly entrained by density-dependent social cues from field-foraging individuals that can override photic entrainment (Fuchikawa et al., 2016). These shifts in temporal rhythms can result both from plasticity in entrainment of the circadian timekeeper and from ‘masking’, or direct environmental modulation of behavioral rhythms outside of the circadian machinery (reviewed by Rivas et al., 2016).

In intertidal and shallow subtidal environments, organisms often show both circatidal (~12.4 h period) and circadian rhythms, with the relative strength of these two rhythms varying both among species and among individuals within a species (reviewed by Bulla et al., 2017). The interaction between tidally-driven and light-driven rhythms can also become complicated when the semidiurnal tides are unequal in magnitude, such that the dominant tidal signal is nearly circadian in periodicity. In addition, both the strength of the tidal signal and the intensity of nocturnal illumination vary as a function of lunar phase, such that semilunar (14.8 day) and lunar (29.6 day) cycles are sometimes observed (reviewed by Naylor, 2010). Studies of transcriptional rhythms and knockdown of core circadian genes have indicated that circadian and circatidal clocks are regulated by largely distinct sets of genes, with the mechanisms of circatidal regulation largely unknown (Takekata et al., 2012; Zhang et al., 2013; Schnytzer et al., 2018).

The sea anemone *Nematostella vectensis* has emerged as a model to study circadian regulation in cnidarians, providing insight into the evolution and diversification of circadian networks in metazoan animals. Studies with lab-reared *Nematostella* have revealed predominantly circadian periodicity in locomotor activity (Hendricks et al., 2012; Oren et al., 2015), although roughly circatidal rhythms have been detected in some individuals (Hendricks et al., 2012). Many of the genes that comprise the core circadian clock in bilaterian animals are also present in *Nematostella*, and some of these show light-entrained diurnal transcriptional cycles (Reitzel et al., 2013b; Oren et al., 2015).

¹Biology Department, Woods Hole Oceanographic Institution, Woods Hole MA 02543, USA. ²Biology Department, University of North Carolina Asheville, Asheville NC 28804, USA. ³Mina and Everard Goodman Faculty of Life Sciences, Bar-Ilan University, Ramat-Gan 52900, Israel. ⁴Biology Department, Boston University, Boston MA 02215, USA.

*Author for correspondence (atarrant@whoi.edu)

 A.M.T., 0000-0002-1909-7899; R.R.H., 0000-0002-5904-1267; O.L., 0000-0002-5478-6307; H.E.R., 0000-0003-4747-1339

Diurnal oscillations in gene expression persist under free-running conditions, although within 2–3 weeks, the signal becomes attenuated or asynchronous among individuals (Peres et al., 2014; Leach et al., 2018). Studies in other cnidarian species, mostly corals, have produced largely consistent results, revealing circadian patterns in gene expression (Hoadley et al., 2011; Levy et al., 2011), with many cyclic genes shared between corals and *Nematostella* (Oren et al., 2015). Sorek et al. (2018) recently provided new insight through analysis of temporal rhythms in the facultatively symbiotic sea anemone *Aiptasia diaphana*. Although both symbiotic and aposymbiotic anemones exhibited diurnal cycles in core circadian genes, only symbiotic anemones exhibited diurnal rhythms in behavior and expression of a wider set of genes. Surprisingly, aposymbiotic anemones exhibited circatidal rhythms in behavior and gene expression, suggesting that the diurnal behavioral and transcriptional rhythms observed in the symbiotic anemones were driven by the presence of symbionts. Lacking a comparable nutritional symbiosis with microalgae, *Nematostella* provides a simpler model of cnidarian chronobiology, and a point of comparison for the work in *Aiptasia*. We sought to determine whether the previously described circadian cycles in *Nematostella* might be an artifact of long-term laboratory rearing and to explicitly test for circatidal patterns. We found that after entrainment in semi-natural field conditions, *Nematostella* retained predominantly circadian behavior patterns and diurnal transcriptional cycles. The regulated genes also point toward a strong effect of light on *Nematostella* physiology, despite their sedimentary habitat.

MATERIALS AND METHODS

Animal culture and field deployment

Nematostella vectensis Stephenson 1935 were originally collected from Great Sippewissett Marsh, Massachusetts (41°35' N 70°39' W) and cultured in the lab over multiple generations spanning several years. They were maintained in Pyrex™ dishes containing filtered natural seawater (from Buzzards Bay, MA) diluted 1:1 with distilled water [to ~16 practical salinity units (PSU)], with a typical density of 50–200 anemones in an 18 cm×13 cm dish with 300 ml diluted seawater. The dishes were housed at 18°C in a walk-in incubator with full-spectrum light provided by 'Reef Sun' bulbs (Zoo Med Laboratories). The daily light–dark cycle was adjusted seasonally, with details provided for each experiment below. Anemones were fed freshly hatched *Artemia* nauplii 4 days per week with weekly to biweekly water changes.

For the gene expression study, 240 *Nematostella* (1–4 cm in length, an unknown mixture of genders and ages) were placed in the field on 16 October 2015. One week prior to deployment, culture conditions were adjusted to match the light cycle (07:00 h sunrise, 18:00 h sunset), and water temperature (19°C) in the marsh. Three days before deployment, animals were conditioned to native marsh water (31 PSU). They were then deployed into a pool within Great Sippewissett Marsh that is known to maintain a natural population of *Nematostella*. The anemones were incubated within 3 cages (80 animals per cage) constructed from large Boyu™ net breeders (Model: NB-3202A, small pens designed for rearing larval aquarium fish). Each cage was constructed from two breeding pens, by assembling one pen, and then using the mesh from the second pen to wrap around the opposite side, covering the opening at the top (Fig. S1). Cages were placed so that they remained fully submerged even at low tide, and secured using zinc-plated steel tent stakes and aluminum rods. Local marsh mud from the upper ~12 cm was filtered through a coarse net (mesh size ~3 mm) to

eliminate large debris, and 250 ml mud/water slurry was added to each cage. Cages were conditioned in the field for 2 days prior to the addition of *Nematostella*. On the morning of 31 October (15 days after deployment), the cages were recovered. *Nematostella* were isolated from the sediments and washed several times in filtered full-strength sea water. Animals were then placed in 6-well plates, 16 animals per well, and these plates were put in the walk-in incubator described above, with a light–dark cycle matched to environmental conditions. Sampling was performed every 2 h over a 24 h period, starting at 17:00 h on 31 October. The short sampling interval was chosen to facilitate detection of circatidal rhythms. At each time point, four replicate samples were collected, each consisting of four pooled animals. For the dark time points, all plates were placed in a covered, dark thick-sided plastic bin to prevent light exposure while entering the room. For sampling, the animals were placed in cryovials, excess water was quickly removed, and vials were snap frozen in liquid nitrogen. During dark periods, this sampling procedure was conducted using only a dim red headlamp. All samples were stored at –80°C until extraction.

Behavioral rhythms were studied in field-acclimatized anemones and compared with anemones maintained in the laboratory ('field' and 'lab' anemones hereafter). Field anemones were deployed into Sippewissett Marsh, as described above, for intervals of 13–21 days spanning 7 October to 17 November 2017 and from 23 May to 15 June 2018 ('autumn' and 'spring', respectively). Cages were similar to those used in the gene expression study but were constructed from smaller breeding pens (Lee Net Breeder larval fish cages; cat. no. 10265; 1 cage per experiment date, 25 animals per cage). The cages containing anemones and sediment were recovered into the laboratory ~10:00 h on the day of assay and allowed to gradually acclimate to room temperature. At ~12:00 h, anemones were isolated from the sediment and washed several times in full-strength seawater. To more closely match the conditions experienced by the field anemones, the lab anemones were transferred to full-strength seawater at least 2 weeks before tracking behavior, and the light cycle was adjusted to approximate field conditions. For behavior experiments, *Nematostella* from both the lab and field groups were isolated into 6-well plates (1 animal per well) with 6 ml full-strength seawater.

Environmental monitoring

In 2015, water temperature in the field was monitored using a HOBO temperature and light logger (Onset Computer Corporation, Borne MA) from 27 October to 16 November, which included the last 4 days of the field deployment for the gene expression experiment. Daily air temperature measurements from Woods Hole, MA (station BZBM3) were retrieved from the NOAA National Ocean Service National Data Buoy Center. Average daily air temperature was strongly correlated with water temperature within the study site ($R^2=0.83$, Fig. S2), so air temperatures were used to estimate water temperature throughout the full deployment. In 2017–2018, water temperature and water depth (HOBO water level logger U20L-04) were monitored throughout the duration of the field deployments. Water depth was calculated from the logged pressure measurements using a reference water depth measured upon deployment and barometric pressure measurements from Station BZBM3. Values below 2 cm were considered unreliable and deleted from the record. Tidal records from West Falmouth Harbor (41.6033°N, 70.6400°W) were retrieved from an online database (<http://tides.mobilegeographics.com/locations/8808.html>). In 2017, salinity was also monitored using a HOBO conductivity logger (U24-002-C).

Behavioral assays

The activity of the anemones in each plate was tracked over a 72 h period using a Daniovision™ observation chamber with an infrared-sensitive camera (DVOC-0040, Noldus Information Technology, Wageningen, The Netherlands). Two independent units were used, allowing two plates to be monitored at the same time. Temperature was maintained at 22°C by an integrated temperature control unit that heated or cooled flowing water surrounding the plate. Field anemones were exposed to either an alternating light–dark cycle (LD), continuous darkness (DD) or continuous light (LL). Lab animals were monitored under LD and DD conditions to enable comparisons with field animals using animals originating from the same laboratory stock and monitored using identical equipment settings. LL conditions were not tested for lab animals because a previous lab study (Oren et al., 2015) and initial results from this field study indicated that circadian cycling is highly reduced under LL. In studies of lab anemones and autumn field anemones, the LD cycle consisted of 11 h of light (07:00 h–18:00 h) and 13 h of darkness (18:00 h–07:00 h), approximating the field conditions during the study period. For the spring field anemones, monitoring was primarily conducted to evaluate behavior under constant conditions (LL and DD). During monitoring of the single spring LD trial, the light cycle consisted of 13 h 20 min of light (06:30 h–19:50 h) and 10 h 40 min of dark; this was inadvertently nearly 2 h shorter than the day length in the field during the entrainment period (05:08 h–20:15 h on 10 June). This was considered a minor issue because it only affected a single trial, and because quantifying the timing of activity peaks was not a primary goal. For all trials, illumination was provided from underneath the plate by an integrated white LED with an intensity of 250 lx (5% of maximum intensity, as in Oren et al., 2015). Activity tracking was conducted using EthovisionXT software (v.12, Noldus Information Technology). Individual wells were defined as tracking ‘arenas’, and movement was tracked using center point detection. Settings were optimized to ensure that anemones were tracked throughout the experiment (imaging rate: 30 frames/min; contour dilation: 2 pixels; contour erosion: 1 pixel; dilate then erode; dynamic subtraction; subject darker than background; contrast: 15–255; frame weight: 2; track noise reduction on). Quality of video tracking was manually assessed at the conclusion of each trial, and erroneous data (i.e. when the software failed to correctly identify the position of the animal) were removed.

The distance moved was summed over each hourly interval and normalized to the maximum hourly distance measured for each anemone (to account for the correlation between size and activity level, as in Oren et al., 2015). Means and standard errors of the normalized hourly values were calculated for all animals within a group (autumn, spring or lab) and light conditions (LD, DD or LL). Edited data series ranged in length from 48 to 96 h; all available time points were analyzed except when specified otherwise. In cases of missing data, the mean and standard error were calculated from the available individual values.

Rhythmicity in locomotor activity was initially assessed through Lomb–Scargle periodogram (‘LSP’ hereafter) analysis as implemented in the R package ‘lomb’ (<https://cran.r-project.org/package=lomb>). For series showing significant periodicity ($P > 0.01$ via visual inspection of plots), period length was assessed using the MFT (mFourfit) algorithm and MESA (maximum entropy spectral analysis) methods as implemented in the BioDare2 web portal (biodare2.ed.ac.uk). Within BioDare2, analyses were constrained to test for periods from 10–14 h (circatidal) or 18–34 h (circadian), depending on the results of LSP analysis. The specific algorithms

used were selected based on recommendations derived from a series of analyses of natural and synthetic datasets of known period and with different waveforms and signal-to-noise ratios (Zielinski et al., 2014). MFT was chosen because it provides an accurate estimate of period that is robust in analysis of short (3 day) time series, similar to the present study. MESA was chosen because it provides a relatively accurate estimate of period and uses a fundamentally different analytical method (curve-fitting by MFF versus stochastic modeling by MESA).

Rhythmicity in gene expression

Total RNA was extracted from pools of 4 anemones using the Aurum Total RNA Fatty and Fibrous Tissue Kit (Bio-Rad) following the manufacturer’s protocol without DNase treatment. RNA quality control, library preparation, sequencing, de-multiplexing, and trimming were conducted by the Genomic Research Center at the University of Rochester. RNA quality was assessed using a Bioanalyzer 2100 (Agilent), producing a mean RNA integrity number of 9.1 and no evidence of genomic DNA contamination. Adapter-ligated libraries were prepared from 48 samples (3–4 per time point) using TruSeq reagents (Illumina). The libraries were sequenced across 6 lanes of an Illumina HiSeq2500 as 100 bp, single-end reads. Sequences were mapped to a *Nematostella* reference transcriptome generated by Helm et al. (2013, see additional file 1 therein). Briefly, Bowtie v.2.2.0 was used to map the trimmed reads using the `–very-sensitive-local` and `–a` flags (settings as in additional file 7 in Helm et al., 2013). Counts were generated from the bowtie output using a python script (additional file 8 in Helm et al., 2013), which filters to count each read only once and remove reads that map to multiple transcripts. To increase statistical power in downstream analyses, the set of counts was filtered to retain only those represented in at least two of libraries and with overall expression of at least 1 count per million. To account for differences in library size, filtered counts were TMM-normalized (trimmed mean of means) within the ‘EdgeR’ R package (Robinson et al., 2010).

Rhythmicity in transcript expression was evaluated using the ‘JTK_Cycle’ R package v3.1 (Hughes et al., 2010). An adjusted P -value of 0.01 was used as threshold for statistical significance. Possible pathways and functions associated with cyclic genes were assessed using gene ontology (GO) enrichment analysis within the R Bioconductor package GoSeq (Young et al., 2010). The most strongly enriched genes were identified based on uncorrected P -values, and a Benjamini–Hochberg false discovery rate of 0.1 was used as a more stringent statistical threshold for enrichment.

Results were compared with two previously published transcriptional profiling studies. The first was a set of 434 transcripts that were upregulated following exposure to ultraviolet radiation (‘UV up’, Tarrant et al., 2018). The second comparison was with a set of 180 transcripts that exhibited a diurnal cycle in a lab-based study in which *Nematostella* were entrained to a 12:12 h LD cycle and then sampled every 4 h over a 48 h period (‘Lab’, Oren et al., 2015).

RESULTS

Behavioral patterns and associated environmental data

To study the effects of field entrainment on *Nematostella* behavior, lab-reared animals were placed in mesh enclosures that were deployed into a pool within Great Sippewissett Marsh. After 13–21 days in the field, *Nematostella* were brought back into the lab. Activity patterns were tracked following autumn field deployments in LD, DD and LL conditions and in lab animals in

LD and DD conditions. Because field conditions became much colder than the lab monitoring conditions later in the autumn, additional spring deployments were conducted followed by monitoring in LD, LL and DD (all raw locomotor activity data are provided in Table S1).

During the autumn field deployments, temperatures ranged from -1.8 to 28.5°C , with a daily average of 14.5°C (2.2 – 24°C range of daily averages; Fig. 1, Table S2). Light measurements in the field showed good agreement with timing of astronomical sunrise and sunset (Fig. S3). While the actual light levels experienced by the sediment-dwelling anemones are unknown, measured light levels near the sediment surface exhibited midday peaks around 5000 lx during deployments in mid-October, and were much higher than the 250 lx used for behavioral monitoring. Tidal variations in water depth occurred as brief (~ 1 h) flooding during high tides around full and new moons (Fig. 1). Depth remained relatively constant during low tides and weaker high tides because the marsh flat separated the pool from the ocean. Over the 42 days of monitoring, 25 flooding events were observed. One of these occurred in association with extremely strong wind gusts during a storm on October 30 and is not considered in further discussions of the relation between tidal height and water depth. The remaining 24 events were distributed over 18 days, and semidiurnal flooding was only observed for brief stretches (6–10 Oct, 17–18 Oct, 3–6 Nov). Flooding tides usually

ranged from 1.40 to 1.71 m, with one occurrence at 1.31 m ($n=24$, mean 1.52 m). Non-flooding tides ranged from 0.95 m to 1.56 m ($n=83$, mean 1.25 m). Tides over 1.43 m usually resulted in flooding (17 out of 25 times, 68% of the time). Salinity usually ranged from 26 to 32 PSU, but the storm at the end of October resulted in a 3 day period of about 17 PSU with a brief drop below 13 PSU. During the spring deployments, temperature ranged from 12.4°C to 36.2°C with an average of 22°C (Table S2). Similarly to the autumn, tidal flooding was brief and associated with high tides around the full moon. Tidal flooding was experienced by the anemones during field entrainment associated with the second and third spring trials, but not the first.

Behavioral rhythms were first characterized using measurements averaged by group (autumn, spring, lab) and lighting condition. Overall, under LD conditions, activity peaked at the beginning of the dark period; however, this increase was absent or reduced on the first night (Fig. 2). Under DD, activity peaks in both groups of field-entrained animals were shifted earlier into late photophase (toward the end of the entrained light-day period), and similarly to observations under LD, the peak at the beginning of the observation period appeared to be suppressed. To explore the effects of disruption during the beginning of observation, LSP analyses were conducted both on the full data series for each group and on series that were truncated to begin at sunrise on the first full day of observations

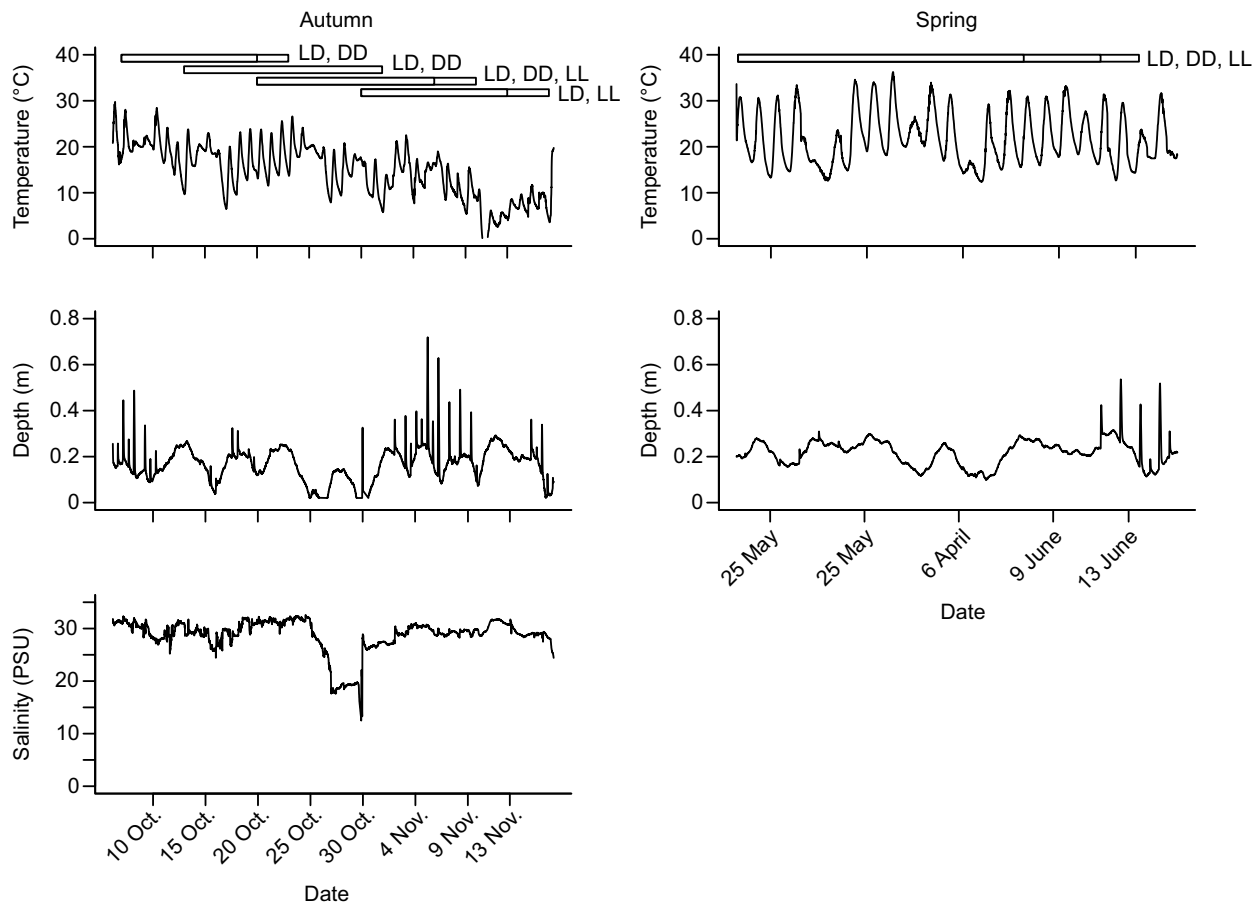


Fig. 1. Environmental parameters over the autumn and spring field entrainment periods prior to behavioral rhythmicity measurements in *Nematostella vectensis*. Note the difference in temporal scale between autumn and spring. Bars at the top indicate the timing of field entrainment for different deployments, with the associated monitoring conditions (LD, DD and/or LL) indicated to the right. In some cases, multiple groups of animals were deployed at the same time and recovered sequentially; the different recovery times are indicated by vertical lines within the bar. Water temperature (top) and sensor depth (center) were measured during both autumn and spring; salinity (bottom) was only measured in autumn. The sensor was deployed near the bottom each time, and the difference between seasons is due to slight differences in deployment position.

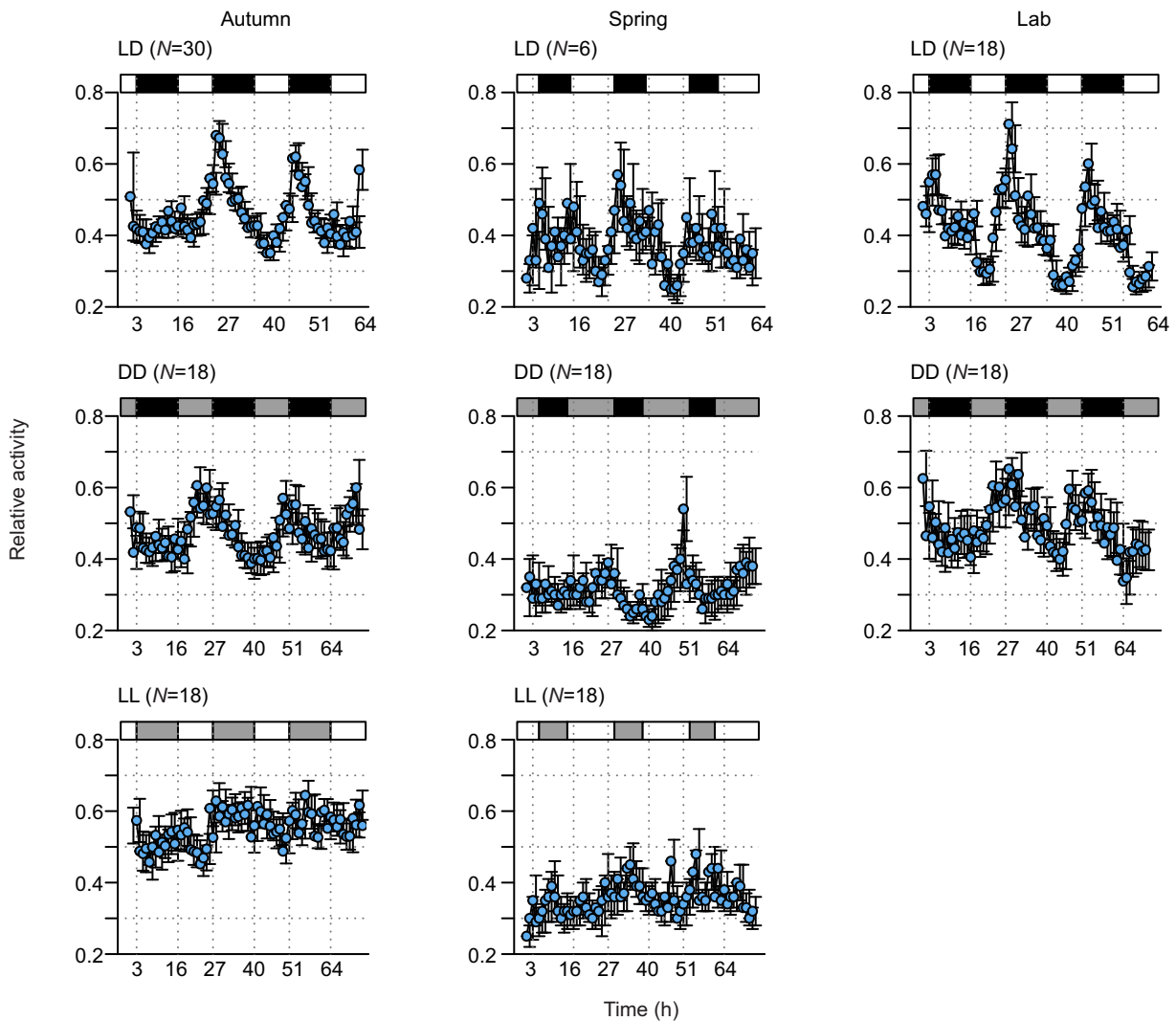


Fig. 2. Normalized plots of activity over a 72 h period under light-dark (LD), constant dark (DD) or constant light (LL) conditions following field or laboratory entrainment of *Nematostella*. *y*-axis shows activity as a proportion of the maximum activity observed for each animal. Bars above plots indicate light daytime (white) and dark night-time periods (black). Gray bars indicate daytime under DD or night under LL. *x*-axis shows hours since start of behavioral monitoring, with label spacing reflecting the timing of light changes in autumn and lab experiments. Plots show mean \pm s.e.m. of tracks from multiple individuals. Sample sizes indicated in Table 1.

(Fig. S4). Within the full data series, significant circadian rhythms were detected under LD and DD conditions in all three groups of anemones (autumn, spring, lab) but not under LL (only autumn and spring were tested). In addition, a significant circatidal rhythm was detected in the lab anemones. In the truncated data series, significant circadian rhythms were detected in all groups and light conditions, but no significant circatidal rhythms were detected. Subsequent analyses

were restricted to the truncated series. While significant circadian periodicity was detected under LL, the rhythm was relatively weak and the circadian peaks in the periodogram analysis had less power than the corresponding peaks in the other light treatments. Estimated periods using three different statistical methods ranged between 23.12 and 27.04 for all groups, with no consistent differences among groups (Table S3).

Table 1. Number (and percentage) of individual *Nematostella* anemones exhibiting significant circadian (20–30 h) or circatidal (10–15 h) periodicity based on LSP analysis

Entrainment	LD			DD			LL		
	<i>N</i>	24 h	12 h	<i>N</i>	24 h	12 h	<i>N</i>	24 h	12 h
Autumn field	30	17 (57)	2 (7)	18	7 (39)	0	18	2 (11)	0
Spring field	6	3 (50)	1 (17)	12	6 (50)	1 (8)	18	1 (6)	0
Lab	18	16 (88)	1 (6)	12	4 (33)	0	0	NA	NA
Total	54	36 (67)	4 (7)	42	17 (40)	1 (2)	36	3 (8)	0

Some anemones exhibited both circadian and circatidal rhythms. $P < 0.01$: see Materials and Methods.

Table 2. Number of transcripts showing diurnal (24 h) and semidiurnal (12 h) cycles at different significance thresholds

	24 h	12 h
BH $Q < 0.05$	347	0
Adj. $P < 0.01$	1640	64
Adj. $P < 0.05$	3813	390

BH Q , Benjamini–Hochberg false discovery rate.

While circadian rhythms were apparent when locomotor activity was averaged by group, rhythmicity was not observed in all individuals within any group (Table 2, individual periodograms available at <https://doi.org/10.6084/m9.figshare.9747632.v1>). Circadian rhythms were most frequently detected under LD and least frequently under LL, which corresponds to the relative strength of the patterns in the averaged data. The lab-entrained LD group had the highest percentage of anemones with circadian rhythms (88%) but overall field- and lab-entrained anemones showed similar proportions. Overall, about 7% of individual (4/54) field anemones showed a circatidal rhythm, and two of these anemones (~4%) exhibited both circatidal and circadian rhythms.

Rhythmic transcript expression

During the field deployment, the animals experienced an estimated average daily water temperature of 11.9°C (4.7 to 17.0°C range of daily averages, Fig. S2). During the last 4 days of the deployment, temperature measurements ranged from 5.0 to 22.8°C, with a daily average of 13.6°C. During the 15 days of deployment, tidal height rose above 1.43 m (likely to cause flooding of the pond, as described above) on 14 occasions, twice daily on each of the last 7 days of deployment.

Transcriptional profiling was conducted on anemones recovered into the lab and sampled every 2 h over a 24 h period. Following mapping of reads to the reference transcriptome, the data set was filtered from the full set of 26,514 to 16,267 of the most abundant transcripts. Within this data set, 1640 transcripts exhibited a 24 h cycle with an adjusted P -value < 0.01 (Table 2 and Table S4). In contrast, only 64 genes exhibited a 12 h cycle.

Of the 1640 transcripts with a diurnal cycle in the present field study, 27 were shared with the 180 transcripts with a diurnal cycle in

a previous lab-based study (Oren et al., 2015; Table 3 and Table S6). The shared genes tended to be strongly cyclic (median rank 45 of 180), have a BLAST-based annotation (17% of annotated versus 5% of unannotated genes shared), and have peak late-night or afternoon expression in the previous study (23% percent of genes in these groups versus 5% of genes in other groups). Shared genes included core circadian regulators (Clock, Cryptochrome 1a) and three chaperone proteins associated with the unfolded protein response (Grp78-like/Hsp70 family, Grp94-like/Hsp90 family and protein disulfide isomerase) (Fig. S5). A Hes/Hey-like transcription factor also exhibited a diurnal cycle in both the lab and field studies. This transcription factor is part of the basic-helix-loop-helix family, has also been found to exhibit diurnal expression cycles in the coral *Acropora millepora*, and has been hypothesized to function as a circadian regulator in cnidarians (Levy et al., 2011; Oren et al., 2015). The probable functions of other shared genes were less clear and included a sortilin-related receptor, DNAJ subfamily gene, collagen, adenosylhomocysteinase and a chloride channel protein.

The phase of the cyclic transcripts was heavily skewed toward maximal expression during the initial daytime sampling points. This is different from the previous laboratory study (Oren et al., 2015), which found a more even distribution of expression patterns. Expression patterns of some strongly cyclic genes were similar between the two studies. For three putative circadian regulatory proteins (Clock, Cryptochrome 1a, Hes/Hey-like; Fig. 3A), both studies found increasing expression around dawn and lowest expression during late night. For core components of the unfolded protein response (Grp78-like, Grp94-like, protein disulfide isomerase; Fig. 3B), both studies found highest expression during the early night and lower expression during late night and daytime.

The transcripts exhibiting a diurnal cycle were also compared with a published set of 434 transcripts that were upregulated following exposure to ultraviolet radiation (UV, Tarrant et al., 2018). Of these, 101 were shared (Table 3 and Table S7). These included genes with known or predicted roles in DNA repair, light sensing, general stress responses, cell signaling and the synthesis of photo-protective compounds. The DNA repair genes included enzymes associated with base excision repair and nucleotide excision repair. Two cryptochrome family members, NvCry1a and Cry-DASH, were also shared between both groups.

Table 3. Selected transcripts with a diurnal cycle that were also identified in previous studies as diurnal or UV-upregulated

Category	Gene name (putative function)	Accession	Lab cyclic	UV-upregulated
DNA repair	NEIL1: Nei-like protein 1 (base excision repair)	v1g13054		✓
	XPC (nucleotide excision repair)	v1g41239		✓
Cryptochrome family	NvCry1a (light sensing, circadian)	v1g168581	✓	✓
	Cry-DASH (DNA repair)	v1g219650		✓
Stress responses	GRP78: glucose-regulated protein 78 (chaperone, unfolded protein response)	v1g216823	✓	
	GRP94: glucose-regulated protein 94 (chaperone, unfolded protein response)	v1g181671	✓	
	PDI: protein disulfide isomerase (chaperone, unfolded protein response)	v1g193399	✓	
	HSP70: heat shock protein 70 (chaperone)	v1g86017		✓
	TSTD1 (thiosulfate sulfurtransferase)	v1g127536		✓
	PHD: pleckstrin homology domain (unknown; metal-induced)	v1g244653		✓
Transcription factors	Clock (circadian regulation)	v1g160110	✓	
	Hes/Hey-like (bHLH family member)	v1g246249	✓	✓
Apoptosis regulation	PDD2L: programmed cell death 2-like	v1g248344		✓
Photo protection	DHQS: 3-dehydroquininate synthase	v1g70416		✓
	HPDL: 4-hydroxyphenylpyruvate dioxygenase	v1g13173		✓
	PdxST: pyridoxal 5'-phosphate synthase	v1g194582		✓
	EGTB: ergothionein biosynthesis protein 1-like	v1g169317		✓
Melatonin synthesis	ASMT: acetyl serotonin O-methyltransferase	v1g91623		✓

Numbers correspond to the accession numbers within the Joint Genome Institute's genomic database <https://genome.jgi.doe.gov/Nemve1/Nemve1.home.html>. The full sets of shared transcripts are listed in Tables S6 and S7.



Fig. 3. Heat maps comparing selected transcriptional profiles between lab-entrained and field-entrained *Nematostella*. Lab data from Oren et al. (2015; 1 replicate derived from 5 pooled anemones per time), and field data from present study (four biological replicates per time). Color scale ranges from red to green (highest to lowest mean relative expression). Time of sampling is shown as Zeitgeber time (ZT), which is the number of hours since sunrise or the start of a light cycle. Black and white bars indicate time points that were sampled during the dark and light phases, respectively. Selected transcripts play putative roles in (A) regulation of the core circadian machinery and (B) the unfolded protein response.

Cryptochromes help to regulate circadian cycles, including through light sensing, and Cry-DASH proteins can have light-dependent DNA repair activity (reviewed by Sancar, 2003). In fact, NvCry1a and the Hes/Hey-like transcription factor were found in all three gene sets.

Among the genes associated with general stress responses, a heatshock protein 70 family member was shared between the sets of UV-induced and rhythmic transcripts. In addition, a pleckstrin homology domain transcript exhibited a diurnal cycle, and was consistently induced in *Nematostella* following exposure to UV (Tarrant et al., 2018), as well as exposure to mercury, cadmium, copper and zinc (Elran et al., 2014). Also present was a potential apoptosis regulator homologous to programmed cell death 2-like (PDD2L). Genes potentially related to photo-protection included those involved in the metabolism of mycosporine-like amino acids and other amino acids (see references within Tarrant et al., 2018). Of these, 3-dehydroquinate synthase (DHQS) catalyzes the second step of the shikimic acid pathway. Ergiothioneine biosynthesis protein 1-like (EGTB) catalyzes synthesis of an alternative aromatic amino acid. 4-hydroxyphenylpyruvate dioxygenase (HPDL), is involved in tyrosine metabolism. Pyridoxal 5'-phosphate synthase (PdxST), catalyzes the synthesis of the active form vitamin B6. This compound serves as a cofactor for many enzymatic reactions, but notably it also can be used as a Schiff base in synthesis of aromatic amino acids through the shikimic acid pathway (Seigler, 1998). Related to hormonal regulation, acetyl serotonin O-methyltransferase (ASMT) catalyzes the final step in synthesis of melatonin.

The 1640 transcripts with a diurnal cycle included several core circadian genes, but after correction for multiple comparisons (FDR<0.1), the only statistically overrepresented GO term was ATP binding (GO:0005524; Table S5). Considering that the GO

enrichment analysis may have been overly stringent, we examined the 20 terms with the lowest uncorrected *P*-values (all <0.0024, Table 4). Two of these were related to GTP hydrolysis, three to post-translational modifications (N-terminal protein amino acid acetylation, protein autophosphorylation, and protein serine/threonine kinase activity) and several to protein folding or preservation (chaperone mediated protein folding requiring cofactor, heat shock protein binding, negative regulation of proteolysis, protein folding, response to unfolded protein). Among the terms with weaker enrichment, 'circadian rhythm' (GO:0007623) had a *P*-value of 0.032, possibly reflecting limitations in transcriptome annotation. For example, the diurnally cyclic genes included two cryptochromes that were not associated with this term, despite the well-characterized roles of cryptochromes in circadian regulation (Chaves et al., 2011).

The transcripts exhibiting semidiurnal periodicity did not include any of the core circadian components or other genes with strong diurnal cycles shown in Table 3. Of the 64 semidiurnal transcripts, 37 were annotated with a total of 150 GO terms, none of which were statistically overrepresented (data not shown). Generally, only one or two transcripts were associated with each term. Three transcripts were associated with 'zinc ion binding', but this term is represented by over 1000 transcripts in the complete data set.

DISCUSSION

Within the field environment, *Nematostella* experienced not only a natural light–dark cycle, but also large daily temperature changes, episodic weather events and seasonal cooling. The dominant rhythm in locomotor activity was circadian in period. Significant circatidal periodicity was relatively rare and observed mainly under LD conditions. Thus, identification of a primarily circadian activity pattern is not an artifact of long-term lab-rearing. Instead it may

Table 4. Most strongly over-represented GO terms among the diurnal cyclic genes in comparison with the full transcriptome

Term	P-value	Diurnal	Total	Description	Class
GO:0005524	4.73E-09	170	1055	ATP binding	MF
GO:0009069	5.80E-05	50	276	Serine family amino acid metabolic process	BP
GO:0005543	2.91E-04	30	144	Phospholipid binding	MF
GO:0060501	4.61E-04	4	5	Positive regulation of epithelial cell proliferation involved in lung morphogenesis	BP
GO:0051085	5.47E-04	5	8	Chaperone-mediated protein folding requiring cofactor	BP
GO:0009986	6.22E-04	22	101	Cell surface	CC
GO:0005083	7.14E-04	7	16	Small GTPase regulator activity	MF
GO:0046777	8.72E-04	22	104	Protein autophosphorylation	BP
GO:0035064	8.77E-04	7	17	Methylated histone binding	MF
GO:0006366	1.02E-03	11	38	Transcription from RNA polymerase II promoter	BP
GO:0043087	1.03E-03	18	75	Regulation of GTPase activity	BP
GO:0006474	1.07E-03	3	3	N-terminal protein amino acid acetylation	BP
GO:0045861	1.18E-03	3	3	Negative regulation of proteolysis	BP
GO:0004504	1.20E-03	3	3	Peptidylglycine monooxygenase activity	MF
GO:0031072	1.31E-03	15	61	Heat shock protein binding	MF
GO:0006457	2.01E-03	19	91	Protein folding	BP
GO:0006986	2.01E-03	6	14	Response to unfolded protein	BP
GO:0004674	2.12E-03	30	169	Protein serine/threonine kinase activity	MF
GO:0003676	2.40E-03	63	428	Nucleic acid binding	MF

Only 'ATP binding' is significantly enriched using an FDR cutoff of 0.1. Full results shown in Table S5.

MF, molecular function; BP, biological process; CC, cellular compartment.

reflect the hydrology of the habitat, which sees only occasional tidal inputs. On the other hand, it has been suggested that circatidal rhythms have greater adaptive value for mobile intertidal organisms such as limpets and isopods, which can relocate and modulate activity in relation to tidal flooding (Naylor, 2010; Schnytzer et al., 2018). Thus, given the limited mobility and subtidal habitat of *Nematostella*, a circatidal rhythm may not be particularly adaptive, even in environments with consistent tidal influence.

While circadian rhythms were observed following entrainment in both the lab and the field, some behavioral differences were associated with the entrainment conditions. In both groups, the activity peak on the first night was either absent or greatly reduced, but the disruption was more notable in the field-entrained groups. For example, the lab-entrained LD group showed a small activity peak on the first night, but the early-morning minimum was comparable to that of the next 2 days. In contrast, the autumn field-entrained LD group showed no peak on the first night and a flat rate of activity through the middle of the first day. Under DD conditions, no peak was observed on the first night in any group, and in both field-entrained groups the first peak was advanced by about 6 h into the first day. A possible explanation for this difference may be the physical disturbance associated with removing the animals from the sediment environment. This could be tested in future laboratory experiments with sediments. We have broadly accounted for this disruption by analyzing truncated datasets; however, future studies should include an acclimation period when animals are brought into the lab prior to beginning behavioral monitoring. A second explanation could be the differences between light, water chemistry and temperature conditions between the field and the lab. In addition, field animals were exposed to natural moonlight, which affects spawning behavior and cyclic gene expression in other cnidarians, notably reef-building corals (Kaniewska et al., 2015; Brady et al., 2016). We also observed considerable individual variability in rhythmicity within each group. While the basis for this variability is not fully known, it may be reduced in future studies by using inbred or clonal lines.

Weak circadian rhythmicity was observed under LL conditions, both in autumn and spring. Significant rhythmicity in mean profiles could only be detected after truncating the initial night of

observation, and significant individual rhythmicity was only detected in a few animals (3 of 36). This result is intermediate between two previously published studies of locomotor rhythms in lab-entrained animals under LL conditions. Oren et al. (2015) found no evidence of significant periodicity under LL. In contrast, Hendricks et al. (2012) observed that after selecting individuals that exhibited rhythmicity in LD, all maintained circadian rhythmicity under LL conditions. The reasons for this discrepancy are currently unclear. Given the substantial variability among individuals, the protocol used by Hendricks et al. (2012) to pre-screen for rhythmicity under LD could help to more specifically test for effects of constant light. In addition, a potential explanation is that the different labs utilized animals sampled from different geographic populations, which may differ in their responses to environmental cues. Oren et al. (2015) used animals derived from the Rhode River Estuary, MD populations established by Cadet Hand (Hand and Uhlinger, 1992; O.L., personal communication), Hendricks et al. (2012) used animals from Charleston, SC, and the present study used animals from Great Sippewissett Marsh, MA. Clines in circadian phenotypes have been documented in diverse animals (Hut et al., 2013). While circadian biology has not been directly compared among *Nematostella* populations, this idea is plausible given that *Nematostella* populations differ in other physiological (e.g. thermal performance, Reitzel et al., 2013a) and behavioral traits (e.g. climbing, H.E.R. and A. Reitzel, personal observations).

The gene expression study corresponded to the behavioral study in the sense that many genes exhibited diurnal rhythms and very few exhibited semidiurnal rhythms. Because the gene expression study was conducted prior to the behavioral studies, it was not known at the time of sampling that behavioral rhythms are disrupted on the first night of monitoring. This may also explain the relatively low concordance (15%) between cyclic genes detected in a previous study and this study. We do not know the effects of these handling artifacts on the transcriptional rhythms within our study, but it is conceivable that the disturbance hindered our ability to detect some truly cyclic genes. One way to avoid such effects in future studies would be to preserve animals immediately after sampling from the field. Despite some possible disruption, the field-entrained animals maintained cyclic expression of several core circadian genes as well

as strongly cyclic transcripts within the unfolded protein response pathway. These shared features indicate that, at least for some genes, transcriptional rhythms are robust.

The diurnally cyclic transcripts substantially overlapped with a set of UV-induced transcripts. Nearly one quarter (23%) of UV-induced transcripts exhibited a diurnal cycle; in comparison 10% of the entire transcriptome exhibited a diurnal cycle. This result implies that solar radiation is physiologically relevant to *Nematostella*. Although these anemones do burrow into sediments, *Nematostella* observed within sediment-filled microcosms typically orient their bodies vertically with the tentacles and mouth positioned above the sediment–water interface (Fig. S1). Emergence from the sediments enables access to planktonic prey and more oxygenated water, but also potentially exposes animals to predators, damaging solar radiation, and strong temperature cycles.

‘ATP binding’ was the most strongly over-represented GO term among the diurnally cyclic genes (Table 4 and Table S5). This is a large and heterogeneous group within the transcriptome (1055 genes, of which 170 exhibited a diurnal cycle) that includes ATP binding cassette proteins, heat shock proteins, myosin and kinases. In a lab-based microarray study of *Nematostella*, Leach et al. (2018) also observed diurnal variation of ‘ATP binding’ genes under both LD and DD conditions. This may reflect an overall cycle in cellular energetics.

Other enriched GO terms were associated with GTP hydrolysis, post-translational modifications and protein folding. GTP often acts as a secondary messenger, including in interactions with G-protein coupled receptors. Differential expression of genes related to GTPase activity has previously been associated with light-entrained diurnal cycles in *Nematostella* (Leach et al., 2018) and lunar spawning cycles in the coral *Acropora millepora* (Kaniewska et al., 2015). Specific post-translational modifications are well-known features of circadian clocks. In protistan clocks, N-terminal acetyltransferase activity is essential for circadian rhythmicity in the green alga *Chlamydomonas* (Matsuo et al., 2012), and autophosphorylation of KaiC is a central component of the cyanobacterial clock (Nishiwaki et al., 2000). Among animals, N-terminal acetylation is a key step in melatonin synthesis (Klein, 2007), some cryptochromes possess autophosphorylation activity (Partch and Sancar, 2005), and the phosphorylation and subsequent degradation of circadian transcription factors is a central component of circadian regulation (reviewed by Brown et al., 2012). Within the present study, a particularly interesting observation was elevated evening expression (centered around sunset ZT11, 18:00 h) of ASMT, the enzyme that catalyzes the final step in melatonin synthesis. This is concordant with previous findings in *Nematostella* of elevated nocturnal levels of both the melatonin hormone and activities of enzymes in the melatonin synthesis pathway (Peres et al., 2014). Among the several highly represented GO terms related to protein folding, components of the unfolded protein response have been consistently observed to exhibit strong diurnal cycles in both corals and *Nematostella*, but the timing of peak expression has differed among studies (Levy et al., 2011; Oren et al., 2015). We consider that the large number of cyclic genes related to protein folding and chaperone activity reflects a large scale daily cycle in translational activity, with the specific timing likely tuned according to the environment. A similar cycle in transcriptional activity may also exist, as suggested by two of the highly represented GO terms: transcription from RNA polymerase II promoter and nucleic acid binding.

Together, the behavioral and transcriptional studies show that circadian rhythmicity persists following field entrainment of

Nematostella. Given the strong daily and seasonal environmental cycles experienced by these animals, future field-based studies could provide additional insight into the coupling of circadian physiology with direct responses to environmental conditions. The diurnal expression of genes related to light sensing, melatonin synthesis and photo protection suggest that solar radiation helps to drive physiological cycles in this sediment-dwelling subtidal animal.

Acknowledgements

We thank D. Brinkley for helpful comments on this manuscript.

Competing interests

The authors declare no competing or financial interests.

Author contributions

Conceptualization: A.M.T., O.L.; Methodology: R.R.H.; Formal analysis: A.M.T.; Investigation: A.M.T., R.R.H., H.E.R.; Resources: A.M.T.; Data curation: A.M.T.; Writing - original draft: A.M.T.; Writing - review & editing: R.R.H., O.L., H.E.R.; Visualization: A.M.T.; Supervision: A.M.T.; Project administration: A.M.T.; Funding acquisition: A.M.T., O.L.

Funding

A.M.T., R.R.H. and O.L. were supported by the Gordon and Betty Moore Foundation (grant number 4598 to A.M.T. and O.L.). H.E.R. was funded by a Martin Family Fellowship for Sustainability at Massachusetts Institute of Technology and an American dissertation grant from the American Association of University Women.

Data availability

All Illumina sequence files have been deposited in the NCBI Sequence Read Archive (BioProject ID PRJNA362308). Individual periodograms are available at <https://doi.org/10.6084/m9.figshare.9747632.v1>.

Supplementary information

Supplementary information available online at <http://jeb.biologists.org/lookup/doi/10.1242/jeb.205393.supplemental>

References

- Brady, A. K., Willis, B. L., Harder, L. D. and Vize, P. (2016). Lunar phase modulates circadian gene expression cycles in the broadcast spawning coral *Acropora millepora*. *Biol. Bull.* **230**, 130–142. doi:10.1086/BBLv230n2p130
- Brown, S. A., Kowalska, E. and Dallmann, R. (2012). (Re) inventing the circadian feedback loop. *Dev. Cell* **22**, 477–487. doi:10.1016/j.devcel.2012.02.007
- Bulla, M., Oudman, T., Bijleveld, A. I., Piersma, T. and Kyriacou, C. P. (2017). Marine biorhythms: bridging chronobiology and ecology. *Phil. Trans. R. Soc. B.* **372**, 20160253. doi:10.1098/rstb.2016.0253
- Chaves, I., Pokorny, R., Byrdin, M., Hoang, N., Ritz, T., Brettel, K., Essen, L.-O., van der Horst, G. T. J., Baschauer, A. and Ahmad, M. (2011). The cryptochromes: blue light photoreceptors in plants and animals. *Annu. Rev. Plant Biol.* **62**, 335–364. doi:10.1146/annurev-arplant-042110-103759
- Elran, R., Raam, M., Kraus, R., Brekhan, V., Sher, N., Plaschkes, I., Chalifa-Caspi, V. and Lotan, T. (2014). Early and late responses of *Nematostella vectensis* transcriptome to heavy metals. *Mol. Ecol.* **23**, 4722–4736. doi:10.1111/mec.12891
- Fuchikawa, T., Eban-Rothschild, A., Nagari, M., Shemesh, Y. and Bloch, G. (2016). Potent social synchronization can override photic entrainment of circadian rhythms. *Nat. Comm.* **7**, 11662. doi:10.1038/ncomms11662
- Hand, C. and Uhlinger, K. (1992). The culture, sexual and asexual reproduction, and growth of the sea anemone *Nematostella vectensis*. *Biol. Bull.* **182**, 169–176. doi:10.2307/1542110
- Helm, R. R., Siebert, S., Tulin, S., Smith, J. and Dunn, C. W. (2013). Characterization of differential transcript abundance through time during *Nematostella vectensis* development. *BMC Genomics* **14**, 266. doi:10.1186/1471-2164-14-266
- Helm, B., Visser, M. E., Schwartz, W., Kronfeld-Schor, N., Gerkema, M., Piersma, T. and Bloch, G. (2017). Two sides of a coin: ecological and chronobiological perspectives of timing in the wild. *Phil. Trans. R. Soc. B* **372**, 20160246. doi:10.1098/rstb.2016.0246
- Hendricks, W. D., Byrum, C. A. and Meyer-Bernstein, E. L. (2012). Characterization of circadian behavior in the starlet sea anemone, *Nematostella vectensis*. *PLoS ONE* **7**, e46843. doi:10.1371/journal.pone.0046843
- Hoadley, K. D., Szmant, A. M. and Pyott, S. J. (2011). Circadian clock gene expression in the coral *Favia fragum* over diel and lunar reproductive cycles. *PLoS ONE* **6**, e19755. doi:10.1371/journal.pone.0019755

- Hughes, M. E., Hogenesch, J. B. and Kornacker, K. (2010). JTK_CYCLE: An efficient nonparametric algorithm for detecting rhythmic components in genome-scale data sets. *J. Biol. Rhythms* **25**, 372-380. doi:10.1177/0748730410379711
- Hut, R. A., Paolucci, S., Dor, R., Kyriacou, C. P. and Daan, S. (2013). Latitudinal clines: an evolutionary view on biological rhythms. *Proc. R. Soc. B* **280**, 20130433. doi:10.1098/rspb.2013.0433
- Kaniewska, P., Alon, S., Karako-Lampert, S., Hoegh-Guldberg, O. and Levy, O. (2015). Signaling cascades and the importance of moonlight in coral broadcast mass spawning. *Elife* **4**, e09991. doi:10.7554/eLife.09991
- Klein, D. C. (2007). Arylalkylamine N-acetyltransferase: the time enzyme. *J. Biol. Chem.* **282**, 4233-4237. doi:10.1074/jbc.R600036200
- Leach, W. B., Marcander, J., Peres, R. and Reitzel, A. M. (2018). Transcriptome-wide analysis of differential gene expression in response to light:dark cycles in a model cnidarian. *Comp. Biochem. Physiol. D Genomics Proteomics* **26**, 40-49. doi:10.1016/j.cbcd.2018.03.004
- Levy, O., Kaniewska, P., Alon, S., Eisenberg, E., Karako-Lampert, S., Bay, L. K., Reef, R., Rodriguez-Lanetty, M., Miller, D. J. and Hoegh-Guldberg, O. (2011). Complex diel cycles of gene expression in the coral-algal symbiosis. *Science* **331**, 175. doi:10.1126/science.1196419
- Matsuo, T., Iida, T. and Ishiura, M. (2012). N-terminal acetyltransferase 3 gene is essential for robust circadian rhythm of bioluminescence reporter in *Chlamydomonas reinhardtii*. *Biochem. Biophys. Res. Comm.* **418**, 342-346. doi:10.1016/j.bbrc.2012.01.023
- Naylor, E. (2010). *Chronobiology of Marine Organisms*. Cambridge University Press.
- Nishiwaki, T., Iwasaki, H., Ishiura, M. and Kondo, T. (2000). Nucleotide binding and autophosphorylation of the clock protein KaiC as a circadian timing process of cyanobacteria. *Proc. Natl. Acad. Sci. USA* **97**, 495-499. doi:10.1073/pnas.97.1.495
- Oren, M., Tarrant, A. M., Alon, S., Simon-Blecher, N., Elbaz, I., Appelbaum, L. and Levy, O. (2015). Profiling molecular and behavioral circadian rhythms in the non-symbiotic sea anemone *Nematostella vectensis*. *Sci. Rep.* **5**, 11418. doi:10.1038/srep11418
- Partch, C. L. and Sancar, A. (2005). Cryptochromes and circadian photoreception in animals. In *Methods in Enzymology* (ed. M. W. Young), Vol. **393**, pp. 726-745. Elsevier.
- Peres, R., Reitzel, A. M., Passamaneck, Y., Afeche, S. C., Cipolla-Neto, J., Marques, A. C. and Martindale, M. Q. (2014). Developmental and light-entrained expression of melatonin and its relationship to the circadian clock in the sea anemone *Nematostella vectensis*. *EvoDevo* **5**, 26. doi:10.1186/2041-9139-5-26
- Reitzel, A. M., Chu, T., Edquist, S., Genovese, C., Church, C., Tarrant, A. M. and Finnerty, J. R. (2013a). Physiological and developmental responses to temperature by the estuarine sea anemone *Nematostella vectensis*: evidence for local adaptation to high temperatures. *Mar. Ecol. Prog. Ser.* **484**, 115-130. doi:10.3354/meps10281
- Reitzel, A. M., Tarrant, A. M. and Levy, O. (2013b). Circadian clocks in the cnidaria: environmental entrainment, molecular regulation, and organismal output. *Integr. Comp. Biol.* **53**, 118-130. doi:10.1093/icb/ict024
- Rivas, G., Bauzer, L. G. S. R. and Meireles-Filho, A. C. A. (2016). "The environment is everything that isn't me": Molecular mechanisms and evolutionary dynamics of insect clocks in variable surroundings. *Front. Physiol.* **6**, 400. doi:10.3389/fphys.2015.00400
- Robinson, M. D., McCarthy, D. J. and Smyth, G. K. (2010). edgeR: a Bioconductor package for differential expression analysis of digital gene expression data. *Bioinformatics* **26**, 139-140. doi:10.1093/bioinformatics/btp616
- Sancar, A. (2003). Structure and function of DNA photolyase and cryptochrome blue-light photoreceptors. *Chem. Rev.* **103**, 2203-2238. doi:10.1021/cr0204348
- Schnytzer, Y., Simon-Blecher, N., Li, J., Ben-Asher, H. W., Salmon-Divon, M., Achituv, Y., Hughes, M. E. and Levy, O. (2018). Tidal and diel orchestration of behaviour and gene expression in an intertidal mollusc. *Sci. Rep.* **8**, 4917. doi:10.1038/s41598-018-23167-y
- Seigler, D. S. (1998). *Plant Secondary Metabolism*. Springer US.
- Sorek, M., Schnytzer, Y., Ben-Asher, H. W., Vered, C. C., Chen, C.-S., Miller, D. J. and Levy, O. (2018). Setting the pace: host rhythmic behaviour and gene expression patterns in the facultatively symbiotic cnidarian *Aiptasia* are determined largely by *Symbiodinium*. *Microbiome* **6**, 83. doi:10.1186/s40168-018-0465-9
- Takekata, H., Matsuura, Y., Goto, S. G., Satoh, A. and Numata, H. (2012). RNAi of the circadian clock gene period disrupts the circadian rhythm but not the circatidal rhythm in the mangrove cricket. *Biol. Lett.* **8**, 488-491. doi:10.1098/rsbl.2012.0079
- Tarrant, A. M., Payton, S. L., Reitzel, A. M., Porter, D. T. and Jenny, M. J. (2018). Ultraviolet radiation significantly enhances the molecular response to dispersant and sweet crude oil exposure in *Nematostella vectensis*. *Mar. Environ. Res.* **134**, 96-108. doi:10.1016/j.marenvres.2018.01.002
- Tomotani, B. M., Flores, D. E. F. L., Tachinardi, P., Paliza, J. D., Oda, G. A. and Valentinuzzi, V. S. (2012). Field and laboratory studies provide insights into the meaning of day-time activity in a subterranean rodent (*Ctenomys aff. knighti*), the tuco-tuco. *PLoS ONE* **7**, e37918. doi:10.1371/journal.pone.0037918
- Vanin, S., Bhutani, S., Montelli, S., Menegazzi, P., Green, E. W., Pegoraro, M., Sandrelli, F., Costa, R. and Kyriacou, C. P. (2012). Unexpected features of *Drosophila* circadian behavioural rhythms under natural conditions. *Nature* **484**, 371. doi:10.1038/nature10991
- Young, M. D., Wakefield, M. J., Smyth, G. K. and Oshlack, A. (2010). Gene ontology analysis for RNA-seq: accounting for selection bias. *Genome Biol.* **11**, R14. doi:10.1186/gb-2010-11-2-r14
- Zhang, L., Hastings, M. H., Green, E. W., Tauber, E., Sladek, M., Webster, S. G., Kyriacou, C. P. and Wilcockson, D. C. (2013). Dissociation of circadian and circatidal timekeeping in the marine crustacean *Eurydice pulchra*. *Curr. Biol.* **23**, 1863-1873. doi:10.1016/j.cub.2013.08.038
- Zielinski, T., Moore, A. M., Troup, E., Halliday, K. J. and Millar, A. J. (2014). Strengths and limitations of period estimation methods for circadian data. *PLoS ONE* **9**, e96462. doi:10.1371/journal.pone.0096462

Table S1: Raw locomotor activity data (cm moved per hour) for all experiments. Note that in all figures and statistical analyses, activity for each animal was normalized (divided) by the maximum hourly activity. The third column (phase of light cycle) corresponds to conditions during the fall and lab studies.

[Click here to Download Table S1](#)

Table S2: Environmental data associated with field entrainment prior to behavioral assays. Average temperature indicates average of daily mean temperature during deployment period.

Deployment	Temperature (°C)		Lunar phase at sampling	Monitoring Condition(s)
	Range	Average		
7 Oct - 20 Oct	6.5 to 28.5	18.2	Recent New (Oct 19)	DD
7 Oct - 23 Oct	6.5 to 28.5	18.2	Crescent Oct 19-27	LD
13 Oct - 1 Nov	6.5 to 26.6	16.2	Gibbous (Oct 28-Nov 3)	LD, DD
20 Oct - 6 Nov	5.8 to 26.6	15.8	Recent Full (Nov 4)	LD, DD
20 Oct - 10 Nov	5.5 to 26.6	14.7	3 rd Quarter (Nov 10)	LD, LL
30 Oct - 13 Nov	-1.8 to 22.5	11.0	Gibbous (Nov 11-17)	LD, LL
30 Oct - 17 Nov	-1.8 to 22.5	10.4	Nearly full (Nov 18)	LL
23 May - 7 Jun	12.4 to 36.2	21.9	3 rd Quarter (Jun 6)	LD, LL
23 May - 11 June	12.4 to 36.2	22.1	3 rd Quarter (Jun 6)	DD, LL
23 May - 15 June	12.4 to 36.2	21.8	Recent New (Jun 13)	DD, LL

Table S3: Period estimates from lab- and field-entrained anemones using the Long-Scargle periodogram (LSP), mFourfit (MFF) and Maximum Entropy Spectral Analysis (MESA) methods.

		LSP	MFF	MESA
Fall	LD	23.42	23.34	23.12
	DD	23.86	24.64	24.02
	LL	23.62	26.16	24.4
Spring	LD	24.22	23.22	23.64
	DD	25.86	25.66	24.72
	LL	27.34	26.8	26.28
Lab	LD	26.78	24.34	25.28
	DD	27.04	26.3	24.92

Table S4: Full results from rhythmicity analysis testing for circadian (columns 2-6) and circatidal (columns 7-10) periodicity. Annotation (columns 11-13) derived from Additional File 7 within Helm et al. 2013. Expression of each replicate shown as TMM-normalized counts (columns 14-61). File sorted according to significance of diurnal cycle.

[Click here to Download Table S4](#)

Table S5: GO enrichment analysis of 1640 diurnal cyclic genes in comparison to the 16,267 genes in the abundance-filtered transcriptome.

[Click here to Download Table S5](#)

Table S6: Intersection between 1640 diurnal cyclic genes in the present field study and 181 diurnal cyclic genes identified in a previous laboratory study. See text for further detail. "Brief annotation" contains brief names subjectively assigned from the blast results to facilitate ease of viewing.

[Click here to Download Table S6](#)

Table S7: Intersection between 1640 diurnal cyclic genes in the present field study and 434 UV-induced genes identified in a previous study. See text for further detail. "Brief annotation" contained brief names subjectively assigned from the blast results to facilitate ease of viewing

[Click here to Download Table S7](#)



Figure S1: Entrainment of *Nematostella* under semi-natural conditions. Top left: mesh cage used in deployments, pen for scale. Top right: example of animal positioned with mouth at the level of the sediment-water interface and tentacles spread across the sediment surface. Bottom: mesh cages deployed within the study site in Great Sippewissett Marsh. See text for additional detail.

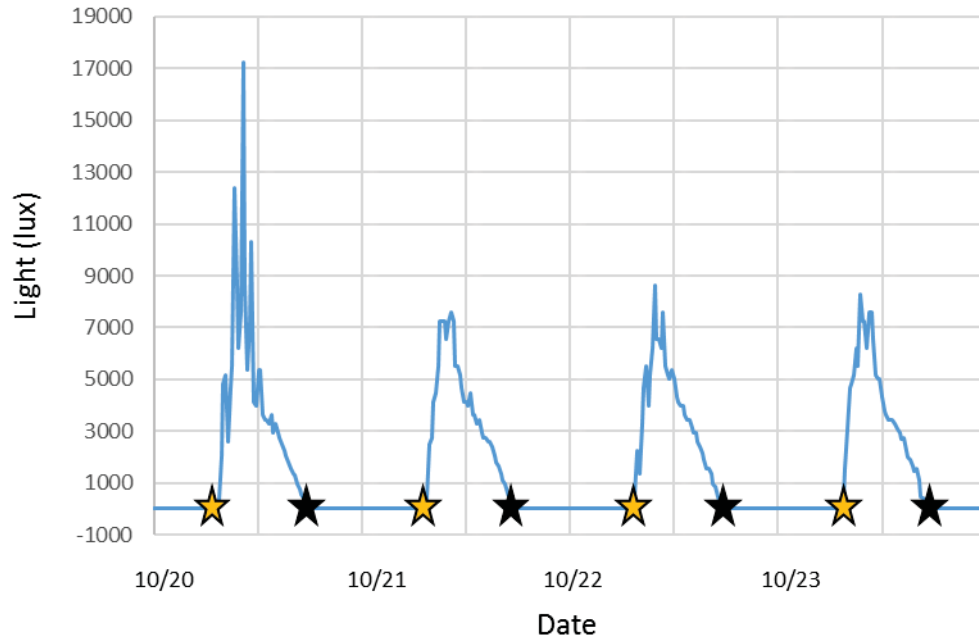


Figure S2: Examples of light levels measured by a HOBO logger during a fall 2017 field deployment. The absolute light levels should be interpreted with caution because the logger dangled in the water column with variable orientation relative to the sun. During this period, the timing of astronomical sunrise and sunset (yellow and black stars) matched within 15 minutes (logging interval) of light levels passing above or below zero lux. Daytime light levels in the water column are much higher than the 250 lux used during behavioral monitoring.

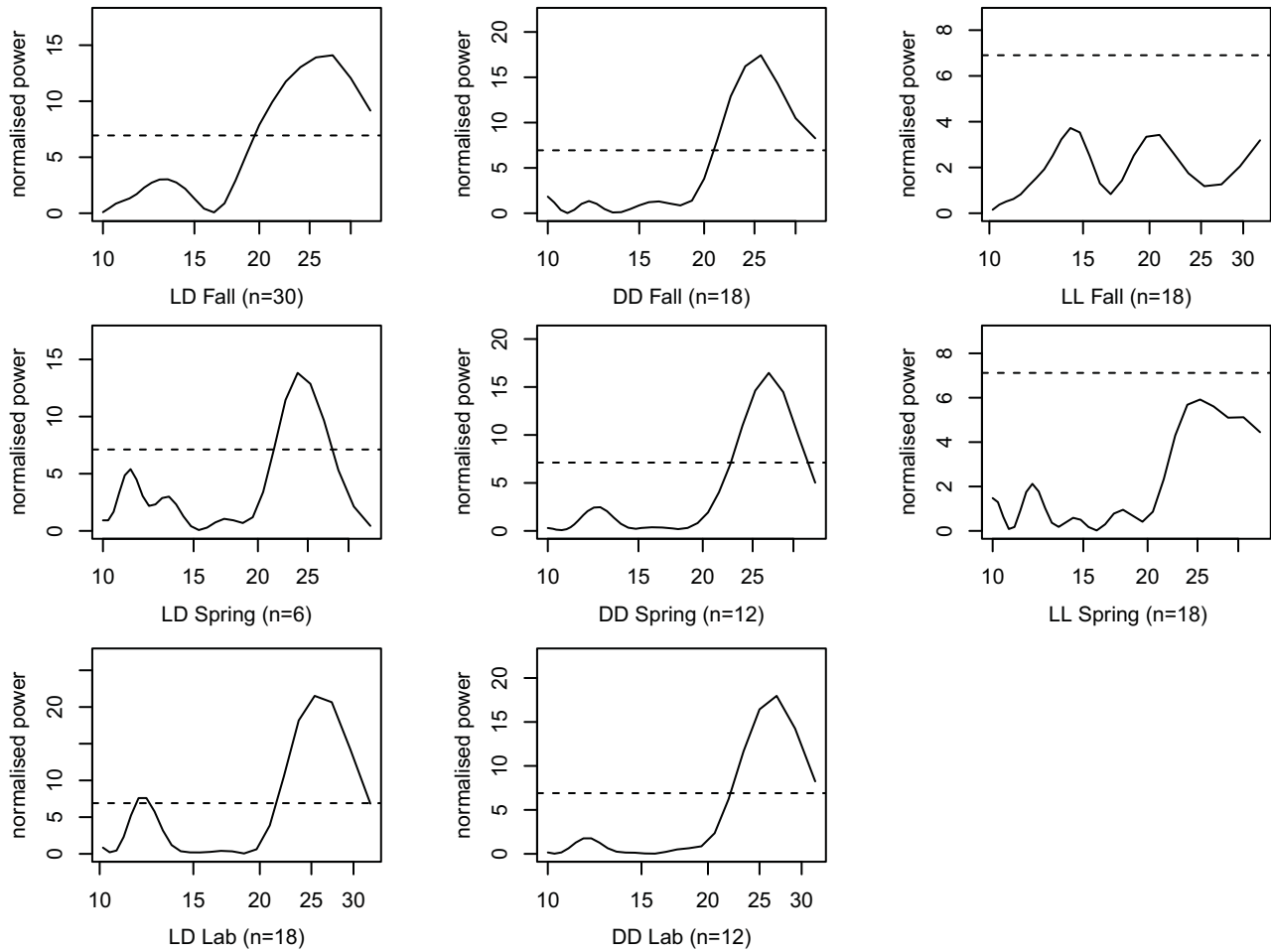


Figure S3: Lomb-Scargle periodogram analysis of full (this page) and truncated (next page) data series averaged across animals entrained in fall field (top), spring field (middle) or lab (bottom) conditions and monitored under LD (left), DD (center) or LL (right). Dashed line indicates significance at $p < 0.01$. In the second set of analyses, series were truncated to begin at sunrise on the first full day of observation.

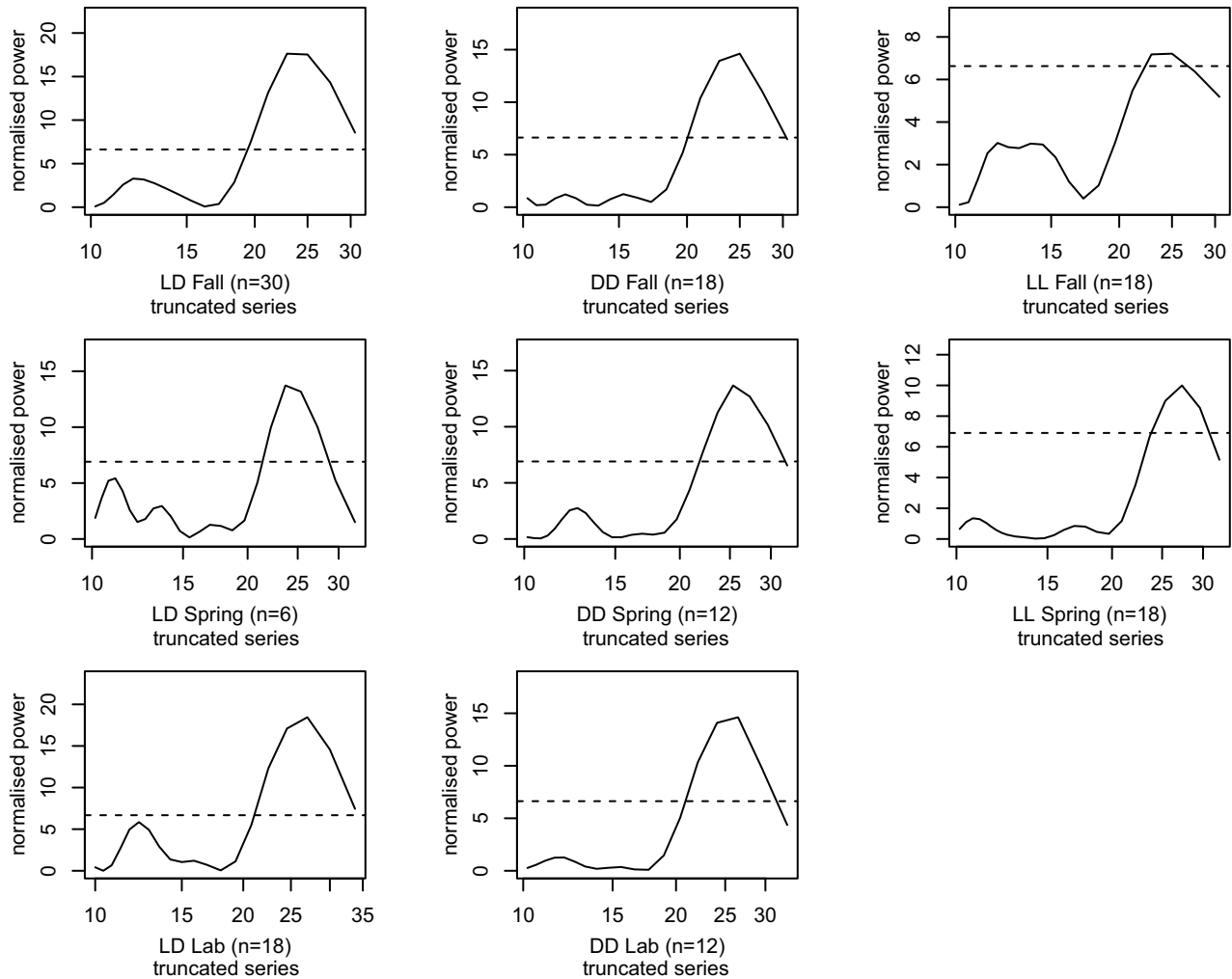


Figure S3: Lomb-Scargle periodogram analysis of full (previous page) and truncated (this page) data series averaged across animals entrained in fall field (top), spring field (middle) or lab (bottom) conditions and monitored under LD (left), DD (center) or LL (right). Dashed line indicates significance at $p < 0.01$. In the second set of analyses, series were truncated to begin at sunrise on the first full day of observation.

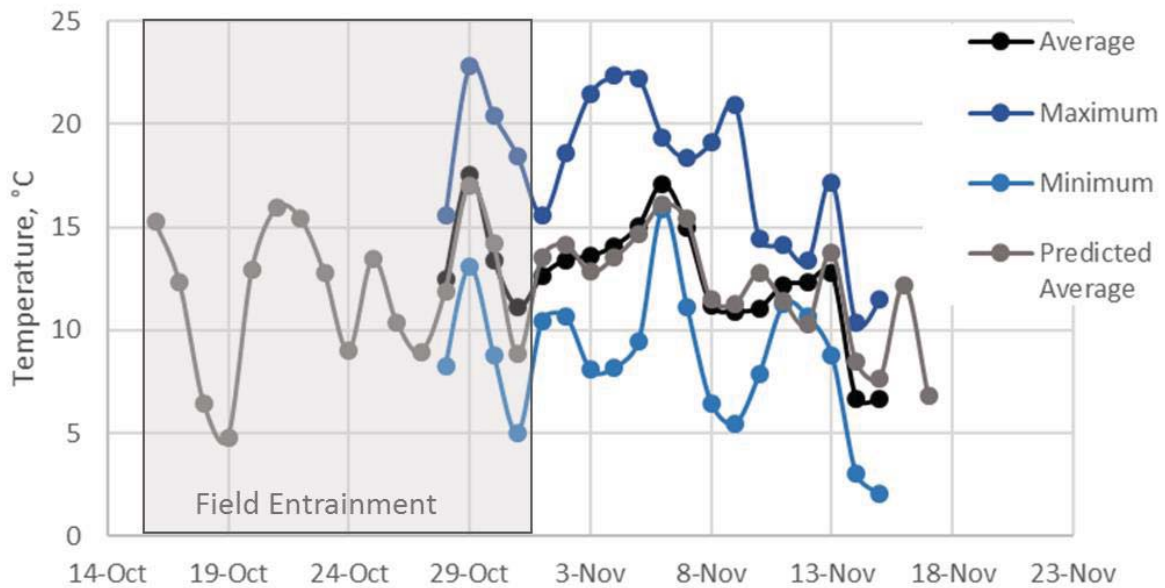


Figure S4: Measured and estimated water temperatures at the field site in Fall 2015. Dark and light blue lines indicate measured maximum and minimum daily water temperatures, respectively. Black and grey lines indicate measured and predicted average daily temperatures, respectively. Temperatures were measured using a HOBO logger and calculated from local air temperature, as described in the text. The shaded grey rectangle indicates the period of field entrainment prior to the gene expression study.

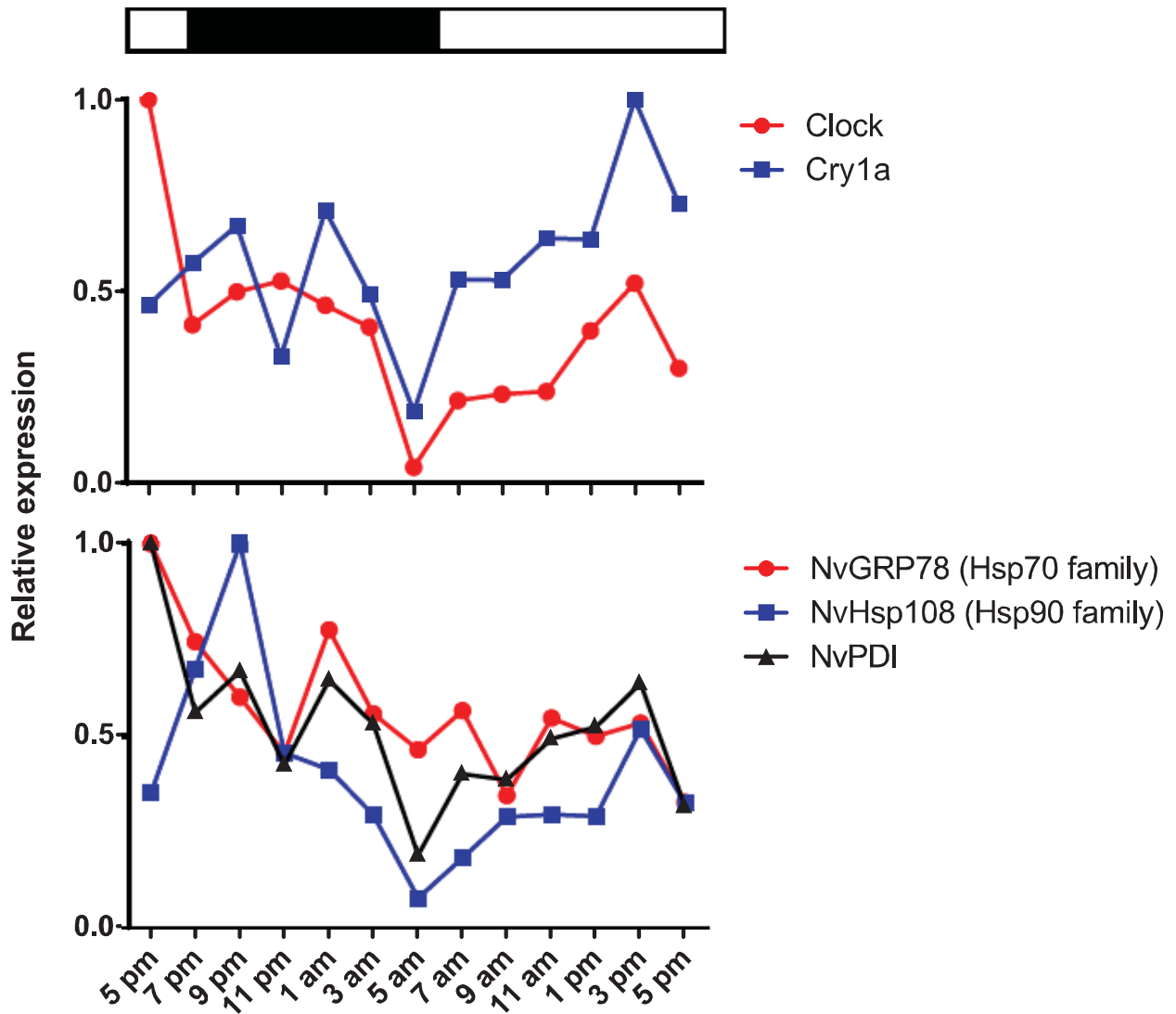


Figure S5: Selected expression profiles of genes with a diel cycle. Top panel shows core circadian regulators, and bottom panel shows three chaperones involved in the unfolded protein response. For each time point, the geometric mean was calculated for the replicate TMM-normalized counts. Expression is represented as a proportion of the maximum value for each gene. The bars at the top indicate light (white) and dark (black) periods.